ATLANTIS PRESS
Atlantis Highlights in Material Sciences and Technology (AHMST), volume 1
International Symposium "Engineering and Earth Sciences: Applied and Fundamental Research" (ISEES 2019)

Solar Concentrator Engineering Design SWx 700-250

Loshkarev I.Yu.
Department of "Engineering physics, electrical machinery and electrotechnology"
Saratov State Agricultural University n. a. N.I. Vavilov
Saratov, Russia
igyulo@mail.ru

Sterkhov A.I.
Technical Director
LLC SOLARGY Group
Izhevsk, Russia
aist@solargy.group

Petrov K.A.
Junior Research Associate
LLC SOLARGY Group
Izhevsk, Russia
constantine_petrov@mail.ru

***Abstract* – The article provides an overview of the effects and phenomena that can be used to accomplish the development of a solar concentrator, the choice of the given physical phenomenon (specular reflection) is presented. Further, technical solutions for this task are developed, the choice of a specific technical solution is justified on the basis of the customer's technical capabilities, and the calculation of geometry of elements of the concentrator on the basis of creation of the course of parallel rays falling at angles from 20^0 up to 90^0 is given. In conclusion, the efficiency of the concentrator on the basis of an increase in the effective area of the light capture is calculated; the calculation of the error of the obtained results is made. From the performed constructions and calculations, it follows that for direct solar radiation (20^0-45^0), the average increase in the values of the effective working area of the light capture was 1.518 times or 51.8%. For diffuse solar radiation (20^0-60^0), the average increase in the values of the effective working area of the light capture was 1.394 times or 39.4%.**

Keywords – natural light; light pipe; light capture; focon; compound-wedged cylindrical concentrator; solar concentrator.

I. INTRODUCTION (*HEADING 1*)

To research and develop a solar concentrator, it is necessary to have an idea of natural light. The section of meteorology that studies radiant energy fluxes in the atmosphere is called actinometry. The only source of natural light is the sun. It emits direct sunlight, part of which dissipates in the atmosphere and creates scattered radiation. Thus, they distinguish the light falling directly from the sun and the light of the "sky" - sunlight scattered by the atmosphere [5, 9, 11].

II. NATURAL LIGHT

Direct solar radiation arriving at the upper boundary of the atmosphere varies over time in small limits, so it is called the solar constant (S_0). An average distance from the Earth to the Sun 149.5•10^6 km S_0 is about 1400 W/m^2 in the energy system of units [1] and approximately 135,000 lx in the lighting system of units. With the passage of a stream of direct solar radiation through the atmosphere, it is attenuated due to absorption (about 15%) and scattering (25%) of energy by gases, aerosols, clouds.

According to Bouguer's law of attenuation, direct solar radiation arriving at the surface of the Earth during a sheer (perpendicular) incidence of rays is as follows:

$$S = S_o \cdot p^m$$

$$\alpha + \beta = \chi$$

. (1) (1)

where p - coefficient of the transparency of the atmosphere; m- the number of optical masses of the atmosphere.

The attenuation of the solar flux in the atmosphere depends on the height of the sun above the horizon of the Earth and the transparency of the atmosphere. The smaller the height, the greater the number of optical masses of the atmosphere that pass the sunbeam. One optical mass of the atmosphere equals the mass, which the rays pass when the sun is in zenith (Figure 1).

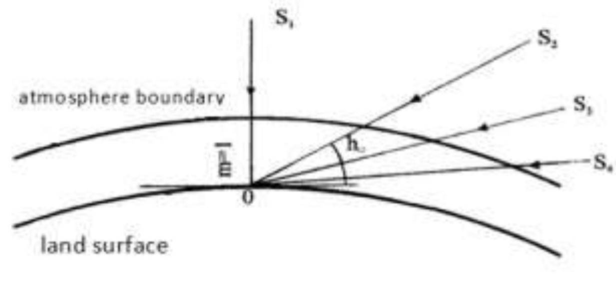

Fig. 1. Diagram of the path of the sunbeam in the atmosphere at different heights of the sun

The longer the path of the sun rays in the atmosphere, the stronger their absorption and scattering and the more their intensity changes.

The transparency coefficient depends on the content in the atmosphere of water vapor and aerosols: the more of them, the less the coefficient of transparency with the same number of passable optical masses. On average, for the whole flow in perfectly clean atmosphere, p at sea level is about 0.9. In actual atmospheric conditions it is 0.7 ... 0.85, in winter it is slightly more than in summer.

In the main agricultural regions of Russia in summer, the midday values of the direct energy radiation illumination are within 700–900 W/m^2 [1]. In general, illumination with direct sunlight varies widely: from 0 lx at sunrise and sunset to several tens of kiloluxes at midday in summer (usually not more than 120 klx). When the height of the Sun changes from 5° to 55°, the direct illumination increases approximately 50 times. The most intensive growth in illumination is observed if the height of the sun is 20 ... 45°. With a sun height of 50°, the illumination of the horizontal surface can reach 55 klx (p = 0.71-0.80), 45 klx (p = 0.61-0.70), 30 klx (p = 0.51-0.60) [1].

Regarding the scattered and total solar radiation, about 25% of the energy of the total flow of solar energy passing through the atmosphere is scattered by molecules of atmospheric gases and aerosols and is converted into scattered radiation in the atmosphere. Scattered radiation comes to the earth's surface not from the solar disk, but from the whole celestial arch. Scattered radiation is different from direct spectral composition, since rays of different wavelengths are scattered to varying degrees.

The maximum of diffuse radiation is usually much less than the maximum of a straight line, but can reach 150-250 W/m^2 [1]. The range of variation of the illumination with diffused light is significantly less than the range of illumination with direct light. The illumination is 0.5 klx at the moments of sunrise or sunset and rises to 13-15 klx at midday hours for average atmospheric conditions. The change in the transparency of the atmosphere has the opposite effect on diffuse illumination compared to direct. With an increase in the turbidity of the atmosphere, the diffuse illumination increases (Figure 2) [2].

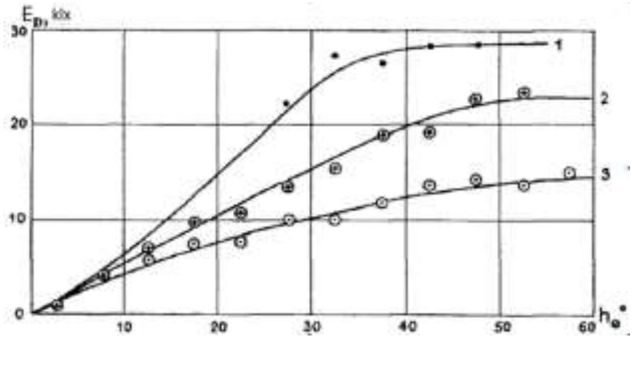

Fig. 2. The dependence of the scattered illumination on the height of the sun for different values of the transparency coefficient (1 - p = 0.5-0.6; 2 - p = 0.61-0.7; 3 - p = 0.71-0.8)

Scattered light increases in cloudy weather by an average of 30%. Snow cover, reflecting up to 70-90% of direct solar radiation, increases diffuse, which is then dissipated in the atmosphere. With an increase in the height of the place on the level of the sea, the scattered radiation with a clear sky decreases. The diurnal and annual variation of the scattered radiation under a clear sky, in general, corresponds to the course of direct emission. However, in the morning scattered radiation appears even before sunrise, and in the evening it still enters the twilight period, i.e. after sunset [1].

Direct solar radiation arriving at a horizontal surface and diffuse solar radiation together make up the total solar radiation. The ratio between direct and scattered radiation in the composition of the total depends on the height of the sun, cloudiness and pollution of the atmosphere. In continuous dense clouds, the total radiation consists entirely of scattered light. In winter, due to the reflection of light from the snow cover and its secondary scattering in the atmosphere, the fraction of scattered radiation in the composition of the total increases noticeably [1]. The relation between the total illumination and the atmospheric transparency factor is small, since the effect of transparency on scattered radiation and the direct one is opposite. The dependence of the total illumination on the height of the sun is very significant (Figure 3) [2].

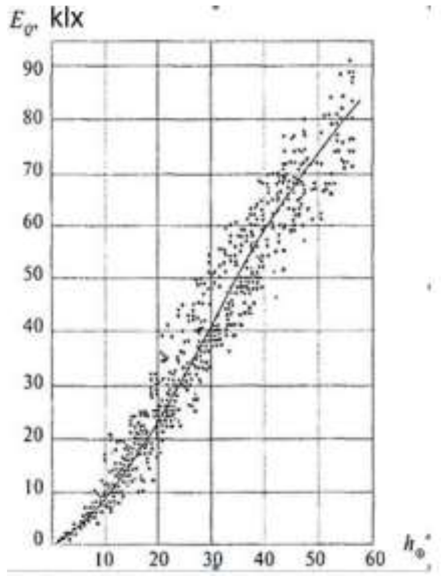

Fig. 3. The dependence of the total illumination of the height of the sun at different values of the coefficient of transparency

III. Methods and Materials

The study and analysis of theoretical and research material lead to the fact that the development of a solar concentrator should be conducted for a certain range of heights of the sun. For direct solar radiation, this is 20 ... 45°, since it is in this range that an intensive increase in illumination is observed according to [2], for scattered radiation it is 10 ... 60° according to [2, 10, 11]. Since it is necessary to obtain the efficiency of the solar concentrator as high as possible, it is advisable that its design could work with both direct solar radiation and diffuse solar radiation.

In general, a concentration system can be defined as a special optical system designed to capture and redistribute the solar radiation flux in space in order to increase its density to the level necessary for further efficient use.

Technically, concentration can be performed using various optical elements - mirrors, lenses, light pipes, etc., however, with the overall dimensions of the light pipe SWx 700-250, it is practically advisable to use mirror reflectors only.

The properties of the systems of concentration of solar radiation describe the geometric and optical characteristics of their reflective surfaces, as well as other indicators. The following basic requirements are imposed on concentration systems:

- high reflectivity in the wavelength range of the spectrum of solar radiation (visible light);
- the consistency of the characteristics of the distribution of concentrated radiation with those required for the effective operation of receiving devices (a mirror tube-light pipe);
- compactness in the transport state with simplicity and reliability of devices;
- the resistance of structural elements and optical coatings of reflective surfaces to the long-term exposure to solar radiation factors (UV resistance);
- low cost and ease of manufacture and repair.

Low-potential solar concentrators can be of two main types with a curved or straightforward generatrix of a reflecting surface. Traditional concentrators of the first type are parabolic cylinders, which are successfully used in ground-based solar installations. Such reflectors with a parabolic generator are called focons (focusing cone) and compound-wedged cylindrical concentrators (Figure 4).

Focons and compound-wedged cylindrical concentrators with a parabolic generatrix have two main positive properties: they do not require high precision manufacturing of the mirror surface of the reflector and, most importantly, retain the original level of concentration of radiation with a low accuracy of orientation of the axis of the reflector.

The sun. In stationary conditions, they can work effectively, remaining stationary for a long time in relation to the star.

The main disadvantage of focons and compound-wedged cylindrical concentrators with a parabolic generator is a significant non-uniformity of the distribution of the density of concentrated radiation, aggravated by the inaccurate orientation of the reflector to the sun.

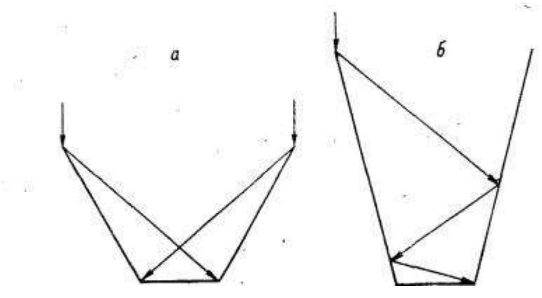

Fig. 4. The scheme of a flat compound-wedged cylindrical concentrator with a single (a) and multiple (b) reflection

This deficiency is significantly less pronounced in reflectors with rectilinear generators or so-called flat compound-wedged cylindrical concentrators [3].

Given there are technical possibilities of manufacturing a concentrator (working only with 2D surfaces) of the customer, as well as the economic aspect, it was decided to develop a concentrator in the form of several focons with a flat generatrix.

The essence of the calculation method was to search for suitable geometric characteristics of the focons (obtained by rotation of generatrixes around a concentrator axis) by constructing a path of parallel rays according to the laws of geometric optics [4, 5, 7]. The sun's rays can be considered parallel at different angles to the mouth of the mirror tube, then, the calculation of the increase in the effective working area of the light capture in relation to the working area of the light capture of the mouth of the mirror tube was made. Data for calculating the effective working area of light capture were determined by the construction of the path of rays, which are constructed using the software package “Compass V12” with an accuracy of 10^{-8} m. By the effective working area, the light capture area of flat focons is meant, after reflection from which the rays enter the mouth of the mirror tube. Constructions and calculations were performed for parallel rays falling on the concentrator at angles: 20°, 25°, 30°, 35°, 40°, 45°, 50°, 60°, 65°, 70°, 75°, 80°, 85°, 90°. The construction of the path of the rays are made for the transverse profile of the SWx 700-250 light pipe. Using the tools of the “Mathcad” software package, the calculated values were interpolated and the values of the increase in the effective working areas of the light capture were obtained for all angles from 20° to 90°.

We consider an example of calculation for parallel rays falling on a concentrator at an angle of 30°. The concentrator geometry was selected so that the concentrator would have the greatest efficiency for the sun rays falling at an angle of 30°, since it is in the middle of the range for both direct sunlight (20-45°) and the scattered one (10-60°).

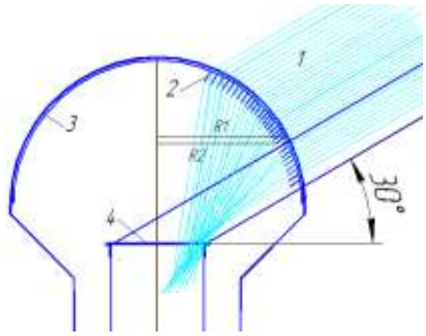

Fig. 5. The path of the rays in the concentrator (1-parallel solar rays; 2 - forming a flat plane of one of the compound-wedged cylindrical concentrators; 3 - protective dome; 4 - mouth of the reflector tube (light pipe))

The geometrical characteristics of the SWx 700-250 light pipe are defined by the customer in the statement of work. They are a limitation for larger R1 and small radii R2 focons. From figure 5 it can be seen that the sun rays falling on the focons at an angle of 30°, after reflection fall into the specular light pipe.

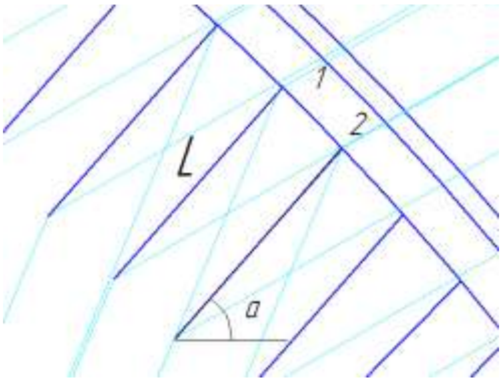

Fig. 6. Reflection of the sun's rays by the focons (L is the length of the forming focon; 1 and 2 are the sun rays; α is the angle of inclination of the forming focon)

The length of the L-forming focon was determined by the fact that ray 1, falling on the upper extreme point of the reflecting surface of the focon, after reflection should fall into the light pipe without obstruction, and ray 2 without obstacles should fall on the lower extreme point of the focon. The focon spacing corresponds to the largest increase in the effective working surface of the concentrator.

After completing the construction of the ray paths, the geometric characteristics of parts of the surface of the focons were determined. After reflection from it the rays fall into the light pipe, namely: the length of the part of the generatrix L, the larger radius R1, the small radius R2, the angle of inclination of the generatrix α to the mirror tube.

	R2 := 0	R1 := 0	L := 0	a := 0
0	125.36	145.06	34.96	55.7
1	142.87	162.57	34.96	55.7
2	159.33	179.03	34.45	55.7
3	173.79	194.86	34.73	52.65
4	186.89	207.96	34.73	52.65
5	199.75	220.76	34.63	52.65
6	211.92	233.05	34.63	52.65
7	224.09	244.94	34.63	52.65
8	233.75	256.69	34.65	48.54
9	242.79	265.74	34.65	48.54
10	251.69	274.63	34.65	48.54
11	259.81	282.75	34.65	48.54
12	...	...	...	...

Fig. 7. Data for the calculation of effective work areas

Figure 7 shows part of the geometric characteristics in mm of each focon. For proper operation in the "Matchcad" environment, it is necessary to convert the tilt angles of the generatrixes to radians. The calculation must be carried out in projection to the light flux. Therefore, it is necessary to determine the angle between the generatrix and the incident ray. The method of translation and the definition of the angle is shown in Figure 8.

Determination of the effective working area of the light capturing for each focon was made using the truncated cone formula, with the resulting angles being multiplied to the received angles to obtain the projection of the generatrixes to the light flux (Figure 9).

```
a_30 := | for i ∈ 0..29
        |   for j ∈ 0
        |     a_i ← (a_{i,j} − 30)·π / 180
        | a
```

$a\_30^T =$

	0	1	2	3	4	5	6	7	8
0	0.449	0.449	0.449	0.395	0.395	0.395	0.395	0.395	...

Fig. 8. Conversion of tilt angles of generatrixes in radians

```
S30 := | for i ∈ 0,1..29
       |   for j ∈ 0
       |     r_i ← π·(R2_{i,j} + R1_{i,j})·(L_{i,j}·sin(a_30_{i,j}))
       | r
```

$S30^T \cdot 10^{-6} =$

	0	1	2	3	4	5	6
0	0.0129	0.0145	0.0159	0.0155	0.0166	0.0176	...

Fig. 9. Determination of effective work areas for each focon (Values of areas are in m^2)

The sum of all values of the effective working areas gives the total effective working area of the concentrator's light capture for the rays falling on it at an angle of 30°.

$$S\_30 := \sum S30 \cdot 10^{-6} = 0.411 \quad м^2$$

Along with the radiation that fell into the mouth of the light pipe through reflection from focons, there is radiation that enters the fiber without reflection, i.e. directly. For such radiation, the calculation of the effective working areas of the light capturing similarly to the reflected flux was also made.

$$S30\_direct\_flow\_SUM := \sum S30\_direct\_flow \cdot 10^{-6} = 0.155 \quad м^2$$

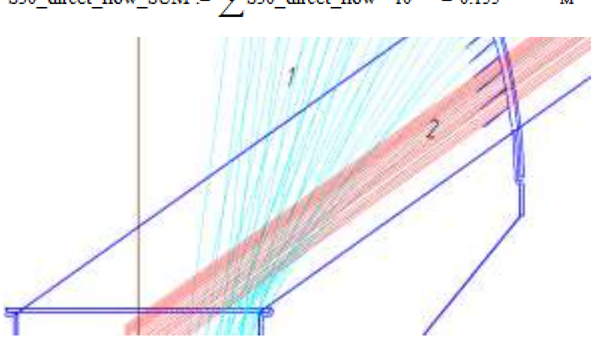

Fig. 10. Passing through the concentrator of the reflected solar flux (1) and direct solar flux (2)

Determination of the effective working area for the mouth of the light pipe is determined as well as for the concentrator. The area of the ball layer (combed cone) is the same area of the mouth of the tube (Figure 11).

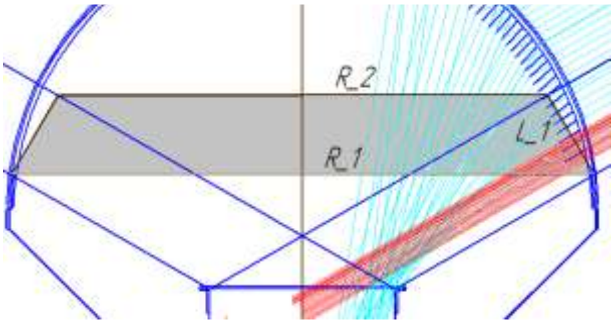

Fig. 11. Determination of the effective working area of the light capture for mouth of the light pipe (R_1 is a small radius; R_2 is a larger radius; L_1 is the length of the projection to the light flux)

$$R\_1 := 334.0$$

$$R\_2 := 396.51$$

$$L\_1 := 125$$

$$S\_optical\_fiber := \pi(R\_1 + R\_2) \cdot L\_1 \cdot 10^{-6} = 0.2869$$

The ratio of the sum of the effective working areas of the focon light capture and the sum of the effective working areas of the light capture of the direct flow to the effective working plane of the light pipe mouth gives an increase in the effective work space of the light capture of the light pipe using a concentrator.

$$total\_area := S\_30 + S30\_direct\_flow\_SUM = 0.566$$

$$Eff := \frac{total\_area}{S\_optical\_fiber} = 1.973$$

The use of a concentrator with these geometric characteristics increases the effective working area of the SWx 700-250 light pipe 1.973 times or by 97.3% for the sunrays falling on the light pipe at an angle of 30°.

A change in the geometric characteristics of the focons leads to a decrease in efficiency, a maximum is reached, since the ray falling at an angle of 30° to any point of the protective dome falls into the mouth of the light pipe.

For angles of 20°, 25°, 35°, 40°, 45°, 50°, similar constructions and calculations were performed. Since the rays falling at an angle of 20° are reflected at a smaller angle and do not fall into the mouth of the fiber on a single reflection, a special apron under the concentrator was designed to redirect the reflected rays to the mouth of the mirror tube (Figure 12).

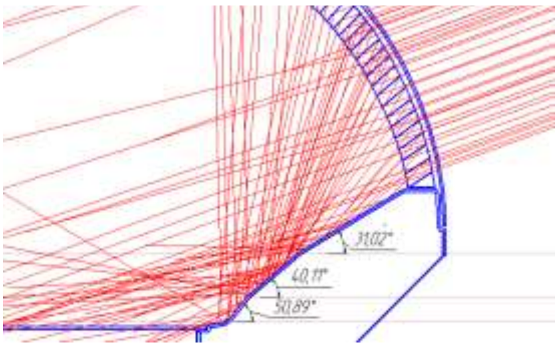

Fig. 12. Optional apron to direct reflected light

The material from which the apron will be made is chosen by the customer on the basis of its technological manufacturing possibilities and economic efficiency. The material must provide a high reflection coefficient and have resistance to yellowing, turbidity when exposed to solar radiation.

For rays falling on the fiber at angles from 60°, the effect of the concentrator is negative. Part of the direct light flow is reflected and derived from the light pipe (Figure 13).

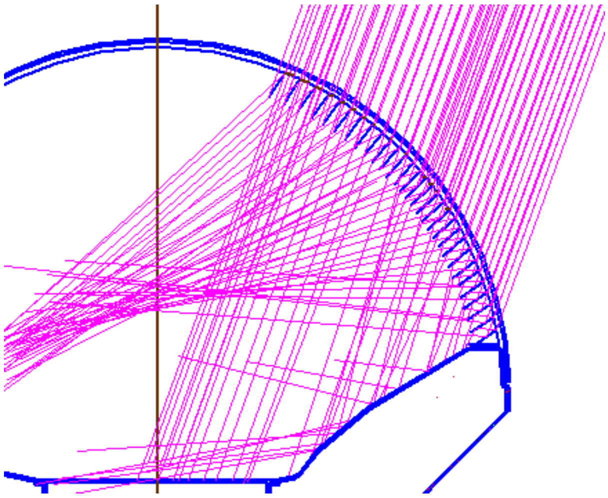

Fig. 13. The path of the rays after reflection in the concentrator for rays falling at an angle of 70°

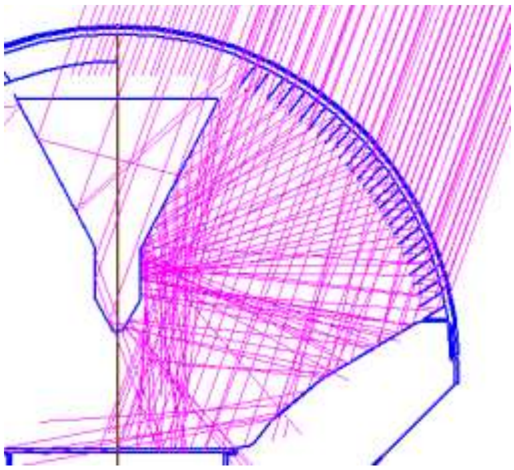

Fig. 14. The path of the rays falling on the concentrator at an angle of 70°, with the addition of a conical reflector

To solve this problem, a special conical reflector was developed. Geometric characteristics are set out in the appendix. The presence in the concentrator of an additional conical reflector increases the effective working area for the radiation incident on the concentrator at angles from 60° to 70° by about 15-20%. The material from which the conical reflector will be made is chosen by the customer on the basis of its technological manufacturing possibilities and economic efficiency. The reflector must be transparent to the solar radiation (visible spectrum) of the material and have resistance to yellowing, turbidity when exposed to solar radiation. It is possible to manufacture the reflector from a matte transparent material, with a transparency coefficient of at least 0.7, since the conical reflector will prevent solar radiation falling below 75 ... 90. Despite the fact that the material is transparent, when radiation is falling on it at angles of 80̊, most of the radiation is reflected (40–100%) [6, 8, 9].

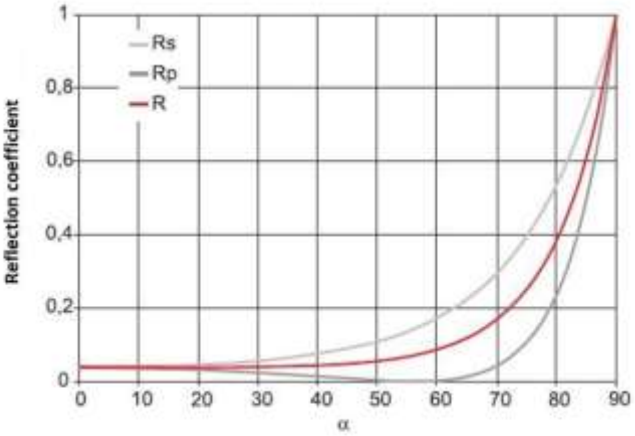

Fig. 15. Reflection from the interface of areas when falling at different angles in accordance with the Fresnel formulas (*Rs* and *Rp* are the reflection coefficients of mutually perpendicularly polarized components of the incident ray, *R* is the total reflection)

Having determined the effective working areas of the light capture for radiation falling at angles of 20, 25,30,35,40,45,50,60,65,75,80,85,90̊, the effective working areas of the light capture for the entire range of angles from 20̊ to 90̊ were determined with the help of the interpolation tools of the "Matchcad" program. Figure 16 presents the data for interpolation, the matrix X is the angle matrix, the matrix Y is the matrix of effective work area values.

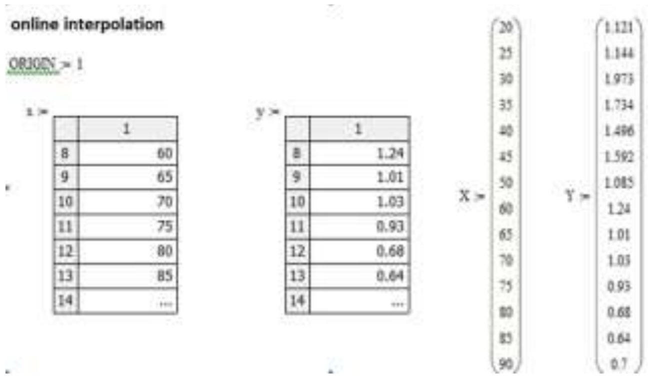

Fig. 16. Interpolation data

Figure 17 shows the values for increasing the effective working area of the light capture for all corners of the range 20 - 90̊, determined with the help of built-in interpolation tools. The table of values of a is the angle values from 20 to 90, for which it is necessary to determine the increase in the area.

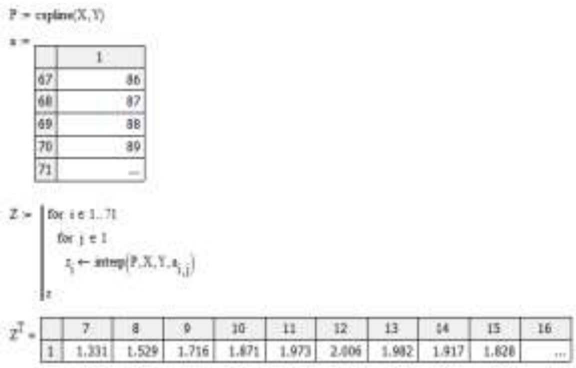

Fig. 17. Determination of increase in effective work areas

On the basis of the data obtained, graphs were constructed to increase the effective working areas of the light capture for each angle in the range of 20-90̊ (Figure 18).

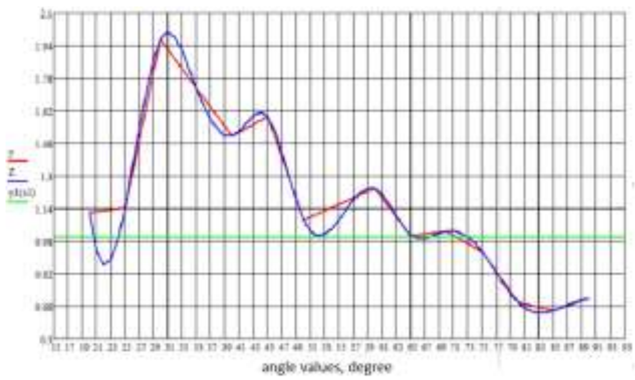

Fig. 18. The graph of the increase in the effective working areas of the light capture (curve Y — obtained on the basis of constructing the path of the rays, curve Z — obtained by interpolation, straight line y1 (x1) corresponds to 1)

From the performed constructions and calculations, it follows that for direct solar radiation (20-45̊), the average increase in the values of the effective working area of the light capture was 1.518 times or 51.8%.

For scattered solar radiation (20̊ – 60̊), the average increase in the values of the effective working area of the light capture was 1.394 times or 39.4%.

IV. Conclusion

In the course of the research the following work was carried out. A review of the effects and phenomena can be used to perform the given task. The choice of the given physical phenomenon is shown and justified (mirror reflection). The review of the existing technical solutions to the given problem, the choice of a specific technical solution based on the technical capabilities of the customer are justified. Calculation of the geometry of the concentrator elements is based on the construction of the course of parallel rays falling at angles from 20̊ to 90̊. Calculation of the efficiency of the concentrator is based on the increase in the effective area of the light capture; calculation of the error of the results. From the performed constructions and calculations, it follows that for direct solar radiation (20̊ -45̊), the average increase in the values of the effective working area of the light capture was 1.518 times or 51.8%. For diffused solar radiation (20°-60°), the average increase in the values of the effective working area of the light capture was 1.394 times or 39.4%.

References

[1] L.S. Polyakova, D.V. Kasharin, Meteorology and climatology. Novocherkassk: NGMA, 2004.

[2] V.A. Semenchenko, Physical Metrology. Moscow: Aspect Press, 2002.

[3] V.A. Griliches, Solar space power stations. Leningrad: Science, 1986.

[4] N.P. Zakaznov, S.I. Kiryushin, V.N. Kuzichev, Theory of Optical Systems. Moscow: Mashinostroenie, 1992.

[5] I.Yu. Loshkarev, O.V. Maletsky, V.I. Loshkarev, N.N. Belova, “The effectiveness of the implementation of light guides for lighting in livestock buildings”, News of the International Academy of Agrarian Education, no. 39, pp. 19–24, 2018.

[6] T.A. Shirobokova, I.Yu. Loshkarev, N.N. Belova, “Methods for assessing the parameters of LED-based lighting in livestock buildings”, News of the International Academy of Agrarian Education, no. 43, pp. 47–50, 2018.

[7] T.K. Mallick, P.C. Eames, B. Norton, “Non-concentrating and asymmetric compound parabolic concentrating building facade integrated photovoltaics: An тexperimental comparison”, Solar Energy, no. 80 (7), pp. 834–849, 2006.

[8] S. Yuehong, B.R. Saffa, P. Gang, “Comparative study on annual solar energy collection of a novel lens-walled compound parabolic concentrator (lens-walled CPC)”, Sus-tainable Cities and Society, vol. 4, pp. 35–40, 2012.

[9] S. Hatwaambo, H. Hakansson, J. Nilsson, B. Karlsson, “Angular characterization of low concentrating PV-CPC using low cost reflectors”, Solar Energy Materials and Solar Cells, no. 92 (11), pp. 1347–1351, 2008.

[10] G. Smestad, H. Ries, R. Winston, E. Yablonovitch, “The thermodynamic limits of light concentrators”, Sol. Energy Mater., no. 21 (2–3), pp. 99–111, 1990.

[11] A. Antonini1, M. Stefancich, J. Coventry, A. Parretta, “Modelling of Compound Parabolic Concentrators for Photovoltaic Applications”, International Journal of Optics and Applications, no. 3 (4), pp. 40–52, 2013.